euronoise

Experimental measurements of the band structure of Lamb waves in phononic lattices

Bernard Bonello, Thomas Brunet and Jiu-Jiu Chen

CNRS and Paris VI University, INSP - 140 rue de Lourmel, 75015 Paris, France
bernard.bonello@insp.jussieu.fr

We have measured the band structure of Lamb waves propagating in 2D phononic crystals. Different cases were investigated. First we have studied the case of phononic slabs with very high contrast between the scatterers and the matrix. The samples are made of 200 µm silicon plates with air holes lattices drilled throughout. Whatever is the symmetry of the lattice, square or centered rectangular, broad band gaps open at first and second reduced Brillouin zone edges. We have also studied the phononic film deposited on a homogeneous substrate. The phononic film is made of cylindrical iron scatterers embedded into a copper background; the substrate is a 700 µm silicon plate. The propagation is along the crystallographic direction [100] of Si. At low filling fraction, a frequency band gap for the antisymmetric mode arises at reduced Brillouin edge. At high filling fraction, a band gap opens also on the symmetric branch. Experimental data are then compared to theoretical predictions obtained using a plane wave expansion method.

1 Introduction

As for the photonic crystals, which are their optical counterpart, there has been during the past few years a growing interest in phononic crystals (PC's). These are artificial media made of a two- or a three-dimensional periodic arrangement of inclusions, embedded in a host matrix (1D periodic structures are a special kind of phononic crystals which is rather called superlattices). It is now well established by a large number of works [1-5], that absolute frequency stop bands may occur in these systems, provided that the elastic properties of the materials making up the heterostructure are sufficiently contrasted. Up to now, most of these works have adopted a theoretical or numerical approach to study these artificial materials and several teams have calculated the band structures of CP's, focusing on the dependence of the stop band(s) on both geometrical parameters (filling fraction, symmetry of the lattice, dimensionality of the CP…) or physical parameters (mass density, elastic constants…). Most of the situations one can imagine have been explored: fluid/solid [6] or solid/fluid [7], solid/solid [8], solid/vacuum [9] …, high [10] or low contrasts [11], bulk [12] or surface acoustic waves [13] propagating in 2D or 3D PC's. In addition to this abundant theoretical activity, several calculation schemes have been proposed: plane waves expansion, finite elements methods, scattering theories and owing to this huge work, the community is now able to anticipate the acoustical response of almost any kind of heterostructure.

Experimental works are less common. In this work, we have used a noncontact experimental technique, based on the use of lasers, for measuring the dispersion curves of Lamb waves propagating in slabs. Indeed, these structures are well suited to confine and to guide the elastic energy in between the free surfaces. Moreover, frequency gaps for both symmetric and anti-symmetric Lamb modes have been theoretically predicted and deserve therefore an experimental investigation. Different situations were explored.

First, we have measured the magnitude of the gaps which opens in the anti-symmetric Lamb mode A0, propagating in PC's exhibiting very high contrasts between the background and the inclusions. The magnitudes of the gaps were measured for different filling fractions and different symmetries. Then, we have tried to answer the question to know whether Lamb waves still undergo band gaps when only the free surface is patterned. To this end, we used the same technique to measure the dispersion curves of samples constituted by a phononic film deposited onto a homogeneous substrate. We then compare the results for different values of the filling fraction.

2 Experiments

2.1 Samples

Three silicon plates (~200 µm thick) were patterned by chemical etching, with air holes arrays drilled throughout). Two samples had the centered rectangular symmetry with different filling fractions, namely $f = 0.21$ and $f = 0.56$ respectively. The third sample had the square symmetry with $f = 0.21$. For each sample, the lattice parameter was $a = 1\,\text{mm}$ and the ratio thickness to lattice parameter $h/a = 0.2$. Note that the chemical etching in silicon is an anisotropic chemical reaction leading to square pyramidal shaped holes (see Fig. 1). We accounted for this particular shape in the calculation of the filling fraction.

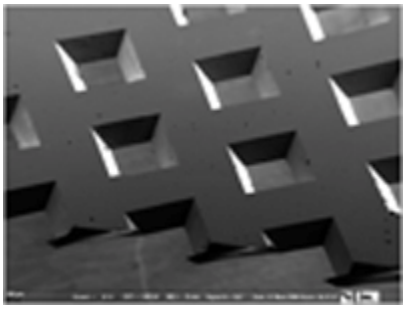

Fig. 1 Image of a silicon/air phononic plate (200 µm thick) with the centered rectangular symmetry.

In addition to these air/silicon samples, we have also elaborated two other samples constituted by a thin 2D patterned film (4 µm thick) deposited onto a homogenous silicon plate (700 µm thick). The structured film was a square lattice of cylindrical iron inclusions embedded into a copper background; the lattice parameter was $a = 1\,\text{mm}$ in both directions of the propagation plane and the filing fractions was respectively $f = 0.25$ and $f = 0.56$. For both types of samples (air/silicon or Fe/Cu film on silicon), the rows of inclusions were parallel to the crystallographic directions [100] and [010] of silicon.

Since our experimental setup allows measuring the dispersion curves of the PC's, recalling the structure in the reciprocal space is important. This is done in Fig. 2 where we show the two first Brillouin zones and the reduced Brillouin zone (shaded area) for the two symmetries we examined. To compute the band structures, we defined a

basis $(O,\mathbf{e_1},\mathbf{e_2})$, with the origin O at the center of an inclusion. For the square lattice of period a, the primitive vectors of the reciprocal space are given as $\mathbf{b_1}:\left(2\pi/a,0\right)$ and $\mathbf{b_2}:\left(0,2\pi/a\right)$. The centered rectangular lattice is deduced from the square lattice by simply translating by $a/2$ along $\mathbf{e}_1$, one row of inclusions over two. This yields the following primitive vectors in the reciprocal space $\mathbf{b_1}:\left(2\pi/a,\pi/a\right)$ and $\mathbf{b_2}:\left(-2\pi/a,\pi/a\right)$. We show also on the left panel of this figure, images of the three air/Si structures under study.

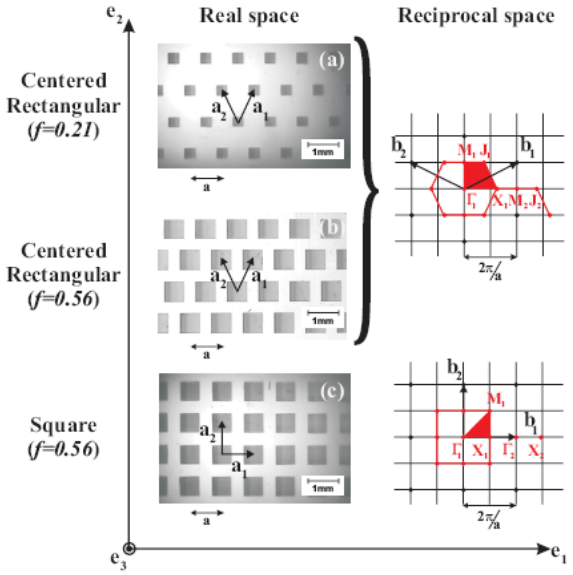

Fig.2 Left panel: images of the three air/Si structures under study defined by the primitive vectors in real space (arrows): centered rectangular arrays with (a) $f = 0.21$, (b) $f = 0.56$ and (c) square array with $f = 0.56$. Right panel: schematic representation of the first (red lines) and of the irreducible (shaded area) Brillouin zones defined by primitive vectors in the reciprocal space (arrows). The coordinates of points Γ_1, X_1, M_2, J_2 for the centered rectangular lattice are respectively (0,0), (5π/4a,0), (2π/a,0), (11π/4a,0). Coordinates of points Γ_1, X_1, Γ_2, X_2 in the square lattice are (0,0), (π/a,0), (2π/a,0) and (3π/a,0) respectively.

2.2 Experimental setup

We used a laser ultrasonic setup to measure the band structures of these PC's. Our experimental technique is based on the laser generation and detection of acoustic pulses with a broad spectrum. Broadband acoustic pulses were generated at the surface of the sample by focusing light pulses issued from a frequency-doubled (532 nm) Q-switched Nd:YAG through a cylindrical lens. The line shaped spot was about 5 mm in long and 70 µm across. In all the experiments described in this article, the excitation zone was located a few millimeters ahead of the PC itself, in a region of the sample free from any air inclusion or iron cylinder.

The time dependence of the surface displacements was recorded at regularly spaced distances from the acoustic source, using a Michelson interferometer in which the light source was a He-Ne laser. One beam of the interferometer was focused on the sample (acting as one of the mirrors of the interferometer) to a spot size of ~15 µm, whereas the reference beam was reflected by an actively stabilized mirror. The interference pattern was collected by a high-speed photodiode and then digitized at 100 MS.s^{-1} by a digital oscilloscope. Both the cylindrical lens and the sample were mounted on translation stages in such a way that the probe beam could be scanned across the sample with a precision of about 1 µm. This noncontact technique allowed us to record the displacement field at any point at the surface of the sample and to resolve hence fine details of the interaction of the acoustic waves with the PC. Note that this interferometric method is only sensitive to the normal component of the displacements but not to the in-plane components.

2.3 Experimental results

We show in Fig. 3 a typical time-space dependence of the normal displacement recorded at the surface of the PC made of a thin phononic film on silicon. The probe beam was focalized on spots regularly spaced at the surface of the PC, in between two consecutive rows of inclusions where the reflectivity of the sample is not modulated. As a consequence of the non-linear dispersion the excited modes, which appear in Fig. 3 as much contrasted colored stripes close to the origin, broaden with increasing position. This is a key feature of elastic modes guided in a plate and clearly suggests that, in the present case, the recorded displacements are actually Lamb waves.

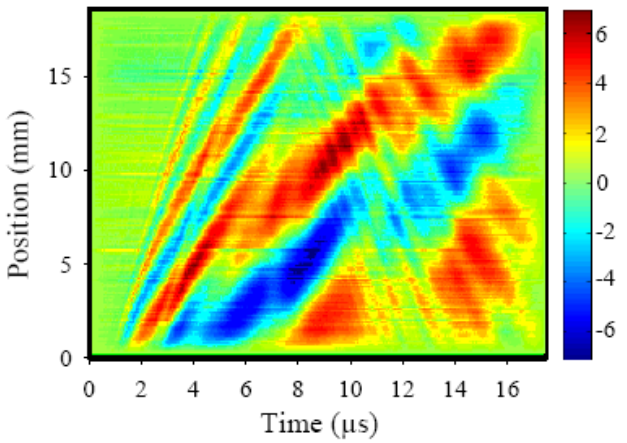

Fig. 3 Displacements field pattern in arbitrary units, recorded at the surface of a 4 µm thick 2D phononic film (iron cylinders embedded in a copper background), deposited onto a silicon plate. The repeat distance in both directions of the plane and the filling fraction are a=1 mm and f=0.25 respectively.

We deduced the dispersion curves of the PC slabs by performing a time-space Fourier transform of the data. We were able to investigate Lamb waves with wave numbers ranging from 0 (Γ in the reciprocal space) to 7000 m^{-1}, beyond the critical point M_2 in the reciprocal space of the centered rectangular array or beyond the point Γ_2 in the reciprocal space of the square network (Fig. 2). The Fourier magnitudes were resolved with accuracies of $\delta\nu$=0.05 MHz for the frequency and δk=300 m^{-1} for the wave number. The

results are displayed in Figs. 4a-b (centered rectangular lattice) and Fig. 4c (square lattice).

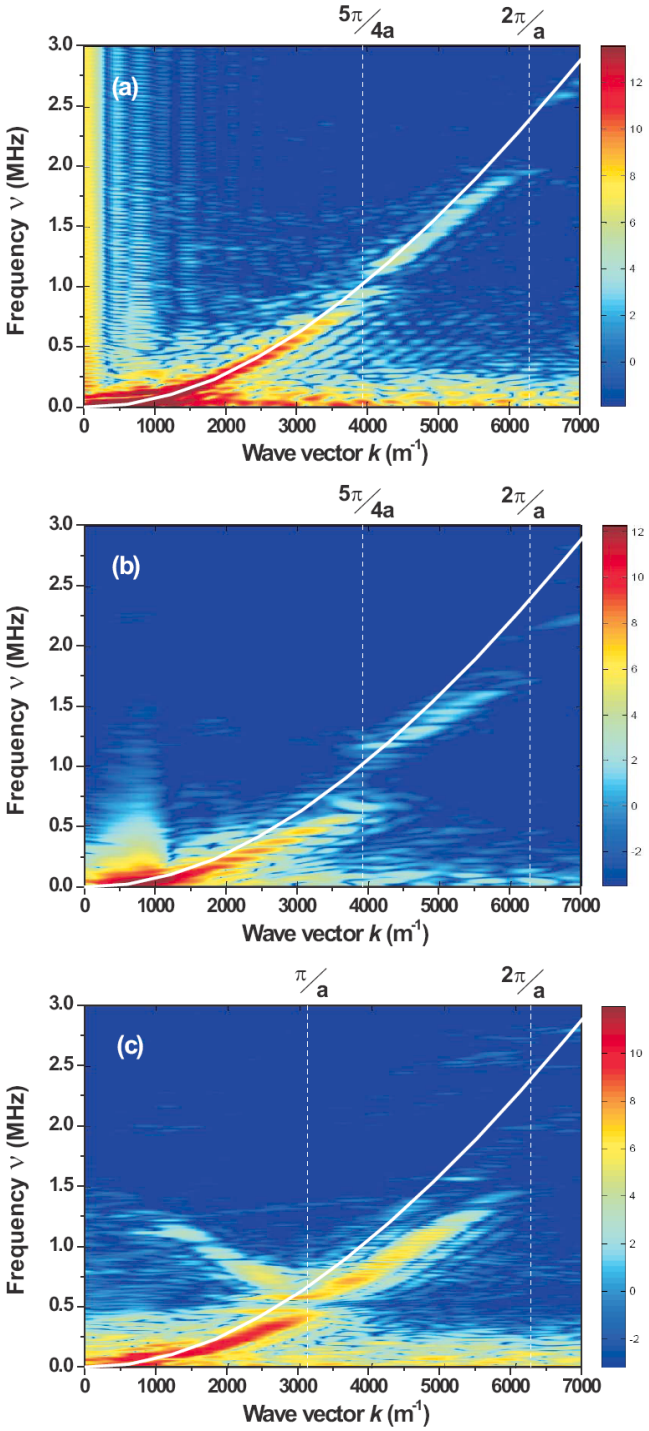

Fig. 4 Experimental dispersion curves along Γ_1-X_1 of the phononic plates deduced through a 2D fast Fourier transform from the measured displacement fields. The color scale is logarithmic. Filling fractions are f=0.21 (a) and f= 0.56 (b) for the centered rectangular array, f= 0.56 for the square array (c). The solid lines are for the calculated Lamb mode A_0 propagating along the crystallographic axis [100] of a 200µm thick silicon homogeneous plate.

Since our detection scheme is based on a Michelson interferometer, it is only sensitive to the out-of-plane component of the ultrasonic waveform. This is the reason why we could only detect the lower order anti-symmetric mode A_0 which has a large out-of-plane component and can therefore be easily observed by the current laser ultrasonic setup. On the contrary, the symmetric mode S_0, while actually excited as well as A_0, cannot be detected. Indeed, in the vicinity of Γ (*i.e.* at low k and low frequency), S_0 is longitudinally polarized. In addition to the dispersion curves of mode A_0, a branch with a negative slope is clearly observable in the range $\left]0, \pi/a\right[$ in Fig. 4c (*i.e.* along Γ_1-X_1).

To understand the nature of this mode, one should remember that our broad band excitation scheme allows for both the excitation and the detection of elastic waves with wave vectors outside the first reduced Brillouin zone. Therefore, folded modes are not expected to appear in the 2D Fourier transforms of the displacements fields; we rather attribute this branche to the signature of elastic waves reflected by the edges of the sample and propagating backward. This is further supported by the measured amplitude of this mode which is about two orders of magnitude less than the one measured along the branche in the range $\left]\pi/a, 2\pi/a\right[$ (*i.e.* X_1-Γ_2), with the same frequencies. Indeed, these backward waves are detected after they have traveled over a distance twice as long as the forward waves and have therefore undergone a strong attenuation through diffusion by the air-holes inclusions.

Another interesting experimental circumstance is when the inclusions have a height much less than the penetration depth of the SAW. In that case, the SAW propagates partly in the periodical structure and partly in the homogenous underlying substrate; the formation of a band gap in the Rayleigh branch has already been predicted [5] in such a system or in the quite similar situation where the surface is corrugated over a depth two order of magnitude less than the wavelength [14] but to the best of our knowledge, it has never been experimentally observed for Lamb waves.

To give experimental evidence for the opening of band gap in Lamb modes for such a system, we have measured the band structures of two PC's, each constituted by a thin 2D patterned film (4 µm thick) deposited onto a homogenous silicon plate (700 µm thick).

The dispersion curves were then obtained by performing a time-space Fourier transformation of the measured displacements. The results are displayed in Fig. 5 where we show in a logarithmic colour scale the Fourier amplitude normalized to unity, as a function of both frequency and wave number in the ΓX direction of the 2D Brillouin zone (corresponding to the propagation along one side of the square unit cell). Five normal modes are observed in the frequency range investigated (0-10 MHz). Indeed, in addition to both lower-order symmetric (labelled S_0) and anti-symmetric modes (labelled A_0), three higher-order Lamb waves with non-zero cut-off frequencies are excited.

We have then computed the dispersion curves of a 700 µm thick silicon uncovered free plate and compared the results to the experimental data (see lines in Fig. 3a). The comparison shows that their overall shapes are not altered by the thin phononic film, as it can be anticipated considering the respective thicknesses of the substrate and the film. Actually, coating the silicon plate with a Fe-Cu layer breaks the symmetry of the problem and strictly speaking, the lower modes are no longer pure symmetric and anti-symmetric Lamb modes. However, for a very thin film on plate, it is expected that the coating affects the

dispersion curves essentially at the centre of the Brillouin zone [16], where the wavelength is much larger than the repeat distance and where, consequently, the phononic film must be treated as an effective medium.

The salient feature in Fig. 5a is the Fourier amplitude of the branch S_0 which cancels to zero for frequencies around 4 MHz and wave numbers $k = 10\pi$ cm^{-1} (see the inset in Fig. 5a). This clearly reveals the opening of a stop band at the edge X of the first Brillouin zone for lower-order symmetric Lamb waves. The measured values of the central frequency and of the width of this stop band are respectively ν=4.2 MHz and $\Delta\nu$=0.6 MHz. No stop band is observed along A_0 or along the higher-order modes for this sample.

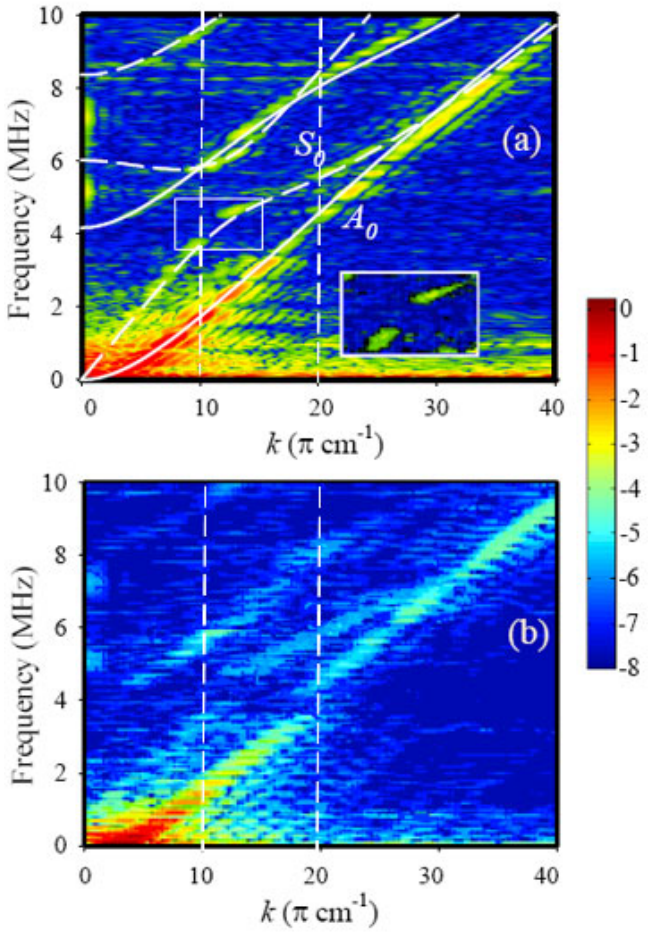

Fig. 5 Experimental dispersion curves along Γ-X of the reduced Brillouin zone, of a thin phononic film on a silicon plate deduced from the data displayed in Fig. 3 through a 2D-FFT. The color scale is logarithmic. The filling fraction are f=0.25 (a) and f=0.56 (b). The lines are for to the calculated Lamb modes propagating along the crystallographic axe [100] of a 700 µm thick silicon plate (full lines: antisymmetric modes; dashed lines: symmetric modes). The parameters used in the calculation are: $\rho_{Si} = 2.329$, $C_{11} = 1.657\times10^{11}$, $C_{12} = 0.637\times10^{11}$ and $C_{11} = 0.799\times10^{11}$ N.m^{-2}. Inset: enlargement of the mode S_0 for frequencies around 4 MHz and $k = 10\pi$ cm^{-1}.

To confirm the opening of a band gap on S_0 and to illustrate the importance of the filling fraction in both its formation and its magnitude, we show in Fig. 5b the measured dispersion curves for the sample at f=0.56. Despite a less good S/N ratio, two gaps are clearly visible for this sample: in addition to the gap on S_0 at $k = 10\pi$ cm^{-1} and ν=4.2 MHz, a stop band comes out now on the branch A_0 at $k = 20\pi$ cm^{-1}, ν=3.9 MHz with a magnitude of about $\Delta\nu$=0.8 MHz. The width of the frequency gap on S_0 is estimated to be $\Delta\nu$=1.3 MHz, about twice as large as for the sample at f=0.25, indicating that the magnitude of the frequency gap behaves against f the same way for Lamb waves and for Rayleigh waves [15].

On the other hand, our data show that the velocities of both symmetric and antisymmetric Lamb waves are those of the uncoated silicon plate. Depending on the filling fraction, frequency gaps appear on the lower-order symmetric and antisymmetric branches, for integer values of the normalised wave vector ka/π and frequencies in the MHz range, as already reported for bending waves in the kHz range [17]. On the other hand, the magnitudes of the stop bands depend on both the geometrical and the physical parameters of the phononic film. This should therefore allow engineering systems in which the central frequency and the magnitude(s) of the stop band(s) are settled on independently and in a controlled way, through a suitable choice of the materials.

References

[1] J. O. Vasseur, B. Djafari-Rouhani, L. Dobrzynski, M. S. Kushwaha and P. Halevi, J. Phys. : Condens. Matter. **6**, 8759 (1994).

[2] M. Kafesaki, M. M. Sigalas and N. Garcia, Phys. Rev. Lett. **85**, 4044 (2000).

[3] T. Miyashita and C. Inoue, Japan. J. Appl. Phys. **40**, 3488 (2001).

[4] T. Miyashita, Meas. Sci. Technol. **16**, R47 (2005).

[5] B. Bonello, C. Charles and F. Ganot, Ultrasonics **44**, 1259 (2006).

[6] Y. Lai and Z.-Q. Zhang, Z. Kristallogr. **220**, 877 (2005).

[7] J. H. Page, S. Yang, Z. Liu, M. L. Cowan, C. T. Chanand and P. Sheng, Z. Kristallogr. **220**, 859 (2005).

[8] B. Bonello, C. Charles and F. Ganot, Appl. Phys. Lett. **90**, 021909 (2007).

[9] R. Martinez-Sala, J. Sancho, J. V. Sanchez, V. Gomez, J. Llinarez and F. Meseger, Nature **378**, 241 (1995).

[10]Y. Tanaka,Y. Tomoyasu and S. Tamura, Phys. Rev. B **62**, 7387 (2000).

[11] C. Charles, B. Bonello and F. Ganot, Ultrasonics **44**, 1209 (2006).

[12] R. Sainidou, N. Stefanou and A. Modinos, Phys. Rev. B **69**, 064301 (2004).

[13] J. J. Chen, K.-W. Zhang, J. Gao and J.-C. Cheng, Phys. Rev B **73**, 094307 (2006).

[14] E. Glass, R. Loudon, and A. A. Maradudin, Phys. Rev. B **24**, 6843 (1981).

[15]Y. Tanaka and S. Tamura, Phys. Rev. B **58**, 7958 (1998).